RSC Advances

ROYAL SOCIETY
OF CHEMISTRY

www.rsc.org/advances

Physicochemical performance of FeCO$_3$ film influenced by anions

Chengqiang Ren[a,b]*, **Wanguo Wang**[b], **Xing Jin**[b], **Li Liu**[b] **and Taihe Shi**[a]

[a] State Key Laboratory of Oil and Gas Reservoir Geology and Exploitation, Southwest Petroleum University, Chengdu, 610500, PR China

[b] School of Materials Science and Engineering, Southwest Petroleum University, Chengdu, 610500, PR China

*Corresponding author. Fax & Tel: +86 28 83037406.

E-mail: chengqiangren@163.com

Abstract: The corrosion film plays an important role in the further electrochemical process of steel in CO$_2$ corrosion. Thus, the physicochemical performance of FeCO$_3$ film was investigated by Mott-Schottky electrochemical technique, potentiodynamic polarization, electrochemical impedance spectroscopy (EIS), X-ray Diffraction (XRD) and scanning electron microscopy (SEM). The performance of FeCO$_3$ film was water chemical dependence. In 0.5 mol L^{-1} NaHCO$_3$ solution, the n-type semiconducting behavior was found for FeCO$_3$ film. The dense microstructure and lower cation interstitial or anion vacancy doping was in favor of strong corrosion resistance of the film. On the contrary, the p-type semiconducting behavior of FeCO$_3$ film was exhibited in both 0.5 mol L^{-1} NaCl solution and 0.5 mol L^{-1} Na$_2$SO$_4$ solution. The

higher cation vacancy doping was found, and the integrity of microstructure was damaged, which decreased the transfer resistance of electron and mass. As a result, the protective ability of $FeCO_3$ film was decreased. The physicochemical mechanism for the semiconducting property of $FeCO_3$ film was explained by the Point Defect Model (PDM).

1. Introduction

CO_2 corrosion of steel has been one of the most important problems in petroleum industry and CO_2 capture process,[1,2] which caused the tubular goods thinning, perforating or fracturing.

Though many different electrochemical mechanisms have been proposed to explain the CO_2 corrosion of steel, the overall reaction is presented as equation (1) :

$$Fe + CO_2 + H_2O \rightarrow FeCO_3 + H_2 \tag{1}$$
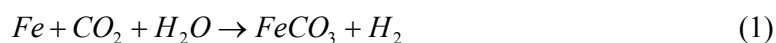
where, $FeCO_3$ precipitates on the surface of steel to form corrosion film, which determines the further corrosion behavior of steel.[3] When referring to the cause of the changes in the corrosion rate, the pitting development, the erosion behavior, etc, many studies have been conducted on the film.[4-6]

The protective ablity strongly depends on the properties of the $FeCO_3$ film on the surface of steel. The first requirement for corrosion inhibition is the integrity of corrosion film. Thus, the mechanical performances of corrosion film, including fracture toughness,[7] wear resistance,[8] Young′s modulus and adhesion strength,[9] have been investigated, and their relations to the protective behaviors were also discussed.

2

The electrochemical behavior of the corrosion film is another important factor to anti-corrosion. The electrochemical characteristic was monitored during corrosion film formation. It indicated the CO_2 corrosion film promoted electrode potential and mass transferring resistance.[10, 11] The passive film on the iron base alloy presented semiconductor property, for example, n-type semiconductor formed on the surface of X70 steel in carbonate/bicarbonate solution.[12] The deep understanding to physicochemical process of the film in electrochemical corrosion can be realized by semiconducting property.

Literatures showed that there was correlation between the corrosion behavior of metal and the semiconducting property of passive film,[13-15] but in CO_2 corrosion field, report was scarcely found. Mott–Schottky measurement is a powerful method to study the semiconductor characteristic. The famous equations are listed as equation (2) for n-type semiconductor and equation (3) for p-type semiconductor according to Mott–Schottky theory:

$$\frac{1}{C_{SC}^2} = \frac{2}{\varepsilon_0 \varepsilon_r N_D A^2}\left(E - E_{FB} - \frac{kT}{e}\right) \qquad (2)$$

$$\frac{1}{C_{SC}^2} = -\frac{2}{\varepsilon_0 \varepsilon_r N_A A^2}\left(E - E_{FB} - \frac{kT}{e}\right) \qquad (3)$$

Where ε_r is the relative dielectric constant of the specimen, which is roughly estimated as 8.0,[16] ε_0 is the permittivity of free space (8.854×10^{-14} F cm^{-1}), e is the electron charge(1.602×10^{-19} C), A is the sample area (cm^2), N_D and N_A are the donor density (cm^{-3}) and acceptor density (cm^{-3}), E_{FB} is the flat band potential (V), k is the Boltzmann constant (1.38×10^{-23} J K^{-1}), and T is the absolute temperature (K).

As our previous work reported, the corrosion of oil tube was severely affected by groundwater chemistry.[17] Generally, anions play important role to the corrosion. In Nesic's review, the species of anions in formation water are Cl^-, HCO_3^- and SO_4^{2-}. For these reasons, the purpose of our work is to clarify the influence of Cl^-, HCO_3^- and SO_4^{2-} to the semiconducting property of $FeCO_3$ film in order to understand the different corrosion behaviors of tubular steel in CO_2 storage oil and gas wells.

2. Experimental

Material

The experimental material is N80 steel with a chemical composition (wt.%) 0.24 C, 0.22 Si, 1.19 Mn, 0.013 P, 0.004 S, 0.036 Cr, 0.021 Mo, 0.028 Ni, and 98.248 Fe. The sample, a plate with a 10×10 mm^2 surface and 3 mm thickness, was machined from the oil tube directly. The pretreatment of the sample included polishing with 800-grit silicon carbide paper, degreasing with acetone, washing with distilled water and drying by blow drier sequentially.

Film preparation

The distilled water was deoxidized by using continuous N_2 bubble adequately (more than 6 h). The pretreated steel samples were hanged separately in the high temperature and high pressure autoclave. The distilled water was pumped into the autoclave till all samples were submerged in the solution. N_2 was bubbled from the bottom of the autoclave for 1 h to further ensure oxygen free. CO_2 were pressured into the autoclave to maintain the total pressure of 8 MPa, and the temperature was heated

4

to 90 ºC. The corrosion film was prepared after 72 h.

Exposure and electrochemical test

The samples were taken out from the autoclave and respectively exposed to three types of solutions including: (1) 0.5 mol L^{-1} NaCl, (2) 0.5 mol L^{-1} Na_2SO_4 and (3) 0.5 mol L^{-1} $NaHCO_3$. All the solutions were prepared by analytical grade reagents and distilled water and deoxidized enough bu N_2 bubble before immersing experiment. The experiment was operated in the airtight five necked flask at 90 ºC. After 72 h exposure, Mott-Schottky electrochemical technique and potentiodynamic polarization were operated in the three conditions. A classical three electrode cell, including a platinum plate counter-electrode, a saturated calomel reference electrode inserted in a electrolytic bridge and a specimen of film covered N80 steel (only 10×10 mm^2 surface exposure), was built for the electrochemical tests. The Autolab Model PGSTAT302N electrochemical potentiostat was used to carry out electrochemical measurements. The Mott-Schottky curve was measured at frequency of 1 kHz and by the potential scan rate of 10 mV s^{-1}. The potentiodynamic polarization was operated by a scan rate of 0.5 mV s^{-1}. EIS measurements were carried out in the 100 kHz to 0.00001 kHz frequency range at open potential, with amplitude of 10 mV peak-to-peak.

SEM and XRD measurement

The phase composition analysis of the prepared film was characterized by a DX-2000 Rigakudmax X-ray diffractometer with a copper Kα X-ray source. The scanning range of 2θ started from 10° to 80°. The JSM-6490LV scanning electron

microscope was used to observe the microstructure of the film.

3. Results and discussion

Prepared FeCO$_3$ corrosion film

Pure FeCO$_3$ corrosion film was prepared successfully in CO$_2$ dissolved distilled water as expected, which was proved by XRD in Fig. 1. All the peaks indicated FeCO$_3$ (siderite) was the sole product. The formation of FeCO$_3$ is regarded as the secondary product of the anodic and cathodic electrochemical reactions when the concentrations of Fe^{2+} and CO$_3^{2-}$ exceed the solubility limit in the local space near the surface of steel. In the various formation waters, all the ions hardly take part in the sedimentary film directly but Ca$^+$.[1, 18] Both CaCO$_3$ and FeCO$_3$ belong to calcite structure, so the trace Ca displaces equivalence number of Fe in the crystal lattice of FeCO$_3$ to produce (Fe, Ca)CO$_3$. This perturbation cannot change the property of the corrosion film. Therefore, the pure FeCO$_3$ film surely represents the corrosion process in the formation water environment.

As can be seen in Fig. 2, the corrosion film was composed of rhombic crystal grains. The compact structure was observed, because the crystal grains arranged in an ordered fashion. The porosity in the film is very low (below 0.1%).[18]

Physicochemical mechanism for semiconducting type

Mott-Schottky curves of FeCO$_3$ film in the three solutions are pictured in Fig. 3 according to the dependence of E and C^{-2}. The electronic conducting behavior can be

analyzed from the Mott-Schottky plot.

The marked difference was observed from the three plots in Fig. 3. In $NaHCO_3$ solution, the positive slope was found, which indicated n-type semiconductor of the film. However, p-type semiconductor of the film was judged from the negative slope in both NaCl and Na_2SO_4 solutions. Thus, the semiconducting property of $FeCO_3$ film is determined by the anion species in formation water.

According to the electron band theory of solid, if the number of electrons in conduction band is more than that of holes in valence band, the solid should be considered as n-type semiconductor. Conversely, it belongs to p-type one. The n-type semiconductor $FeCO_3$ film is contributed to the doping of cation interstitial or anion vacancy. The doping of cation vacancy in the $FeCO_3$ film makes it present p-type semiconductor.

Referring to the PDM resulted from the research group of Macdonald,[19] the physicochemical process of $FeCO_3$ film in different solutions was described schematically in Fig. 4. PDM-II is suitable to explaining the corrosion film by precipitation of ferrous ion with carbonate ion. The semiconducting property of $FeCO_3$ film is determined by the complex process of generation, diffusion and annihilation of charge carrier.

It is well known that seven basic reactions occur in the steel/film/solution system as seen in Fig. 4 labeled as (I) to (VII). Various anions have different influences to these reactions by the diverse adsorptive and reactive abilities. Reactions (I), (IV), (VI) and (VII) present at the interface of the outer layer of $FeCO_3$ film and solution

(film/solution), the other reactions occur at the interface of steel and the inner layer of FeCO$_3$ film (steel/film). Here, symbols are cation vacancy, V_{Fe}^{2-}, anion vacancy, V_O^{2+}, cation interstitial, Fe_i^{2+}, neutral vacancy, V_{Fe}, ferrous ion in cation site, Fe_{Fe}, anion ion in anion site, $[O]_o$, hydration anion, $X^{x-} \cdot nH_2O$, film forming anion, $[O]$, aqueous ferrous ion, $Fe(H_2O)_n^{2+}$, and film compound, $Fe[O]$.

The V_{Fe}^{2-} generates according to reaction (I) by adsorption of $X^{x-} \cdot nH_2O$ to the active Fe_{Fe} in the FeCO$_3$ film. Cation vacancy is regarded by the catalysis of adsorbed species.[20] The following step is the diffusion of V_{Fe}^{2-} from film/solution towards to steel/film. The V_{Fe}^{2-} eliminates in reaction (II). The V_O^{2+} and Fe_i^{2+} are produced by reactions (III) and (V). After diffusion to the surface of film, they disappear by reactions (IV) and (VI). Reaction (VII) means the dissolution of the film.

Guo et al. believed that FeCO$_3$ had strong adsorption to anion via Coulombic as well as Lewis acid–base interactions.[21] Among HCO$_3^-$, SO$_4^{2-}$ and Cl$^-$, the former is softer than the latter two in Lewis acidity on the basis of "hard and soft acid and base" concept,[22] so adsorption ability of HCO$_3^-$ to the same base Fe^{2+} in the film is weaker than SO$_4^{2-}$ and Cl$^-$. Literatures reported Cl$^-$ and SO$_4^{2-}$ played an important role on the corrosion products of iron to form complex compounds.[23, 24] It could be supposed that transient products of FeCO$_3$Cl$^-_{ads}$ and FeCO$_3$SO$_4^{2-}{}_{ads}$ present in the film due to the adsorption of Cl$^-$ and SO$_4^{2-}$ to Fe_{Fe} in the film, where, the subscript "ads" means adsorption state. The adsorption to the film was found by XPS as M-O-X bond.[25] The amount of V_{Fe}^{2-} caused by reaction (I) in NaHCO$_3$ solution is much less than in Na$_2$SO$_4$ and NaCl solutions.

The kinetics of reaction (IV) is also affected by the $X^{x-} \cdot nH_2O$, thus, the amount of consumed Fe_i^{2+} in Na_2SO_4 and NaCl solutions is more than in $NaHCO_3$ solution. The annihilation of V_O^{2+} runs in two ways as reaction (VIa) and reaction (VIb). Reaction (VIa) indicates the anion, HCO_3^-, is favor of $FeCO_3$ film formation, reaction (VIb) yet cannot precipitate solid production by anion, such as SO_4^{2-} and Cl^-. The adsorbed anion X^{x-} will be trapped by V_O^{2+}. The anion occupies the V_O^{2+} leading to further reactions. When it meets with V_{Fe}^{2-}:

$$X_O^{2-x} \cdot nH_2O + \frac{2-x}{2}V_{Fe}^{2-} \rightarrow nH_2O + Null \tag{4}$$
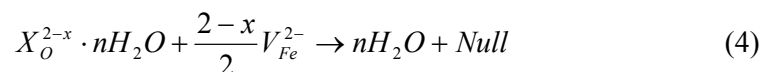
However, when it reacts with neighboring Fe_{Fe}:

$$X_O^{2-x} \cdot nH_2O + Fe_{Fe} \rightarrow Fe(H_2O)_n^{2+} + \frac{1}{x}\left[V_{Fe}^{2-} \cdot V_O^{2+}\right] \tag{5}$$
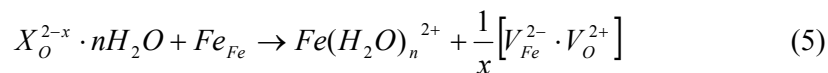
Therefore, HCO_3^- takes part in the film formation resulting in more dense structure. On the other hand, adding $NaHCO_3$ elevates the pH of solution because of its strong base and weak acid performance, which mitigates solubility of iron carbonate. SO_4^{2-} and Cl^- yet lead to porous structure based on soluble ion of $Fe(H_2O)_n^{2+}$ produced in several reactions. The anions adsorbed on the film undergo hydrolysis and reduce the local pH, which also causes the dissolution of film. The microstructure can be affirmed by Fig. 5. The SEM images of the $FeCO_3$ film surface after 72 h immersion in $NaHCO_3$, Na_2SO_4 and NaCl solutions was shown in Fig. 5. The shape and arrangement of crystals in $NaHCO_3$ solution were similar to the initial $FeCO_3$ film prepared from CO_2 dissolved distilled water. However, the surface morphology became porous after immersing in the other two solutions, and the crystalline grain changed to spherosome.

Cl⁻ is a well known corrosion accelerator to metal in aggressive environments. The role of SO_4^{2-} is not well clarified. It has been found that SO_4^{2-} was more aggressive than Cl⁻, and SO_4^{2-} was the specie responsible for pitting attack to copper.[26] During formation of artificial steel rust particles prepared from acidic aqueous Fe(III) solution, the influence of SO_4^{2-} is more important than Cl⁻.[24] Deng et al suggested that SO_4^{2-} would supplant the adsorbed Cl⁻ and accelerate effect of pitting initiation.[27] Thus, SO_4^{2-} indeed is a strong aggressive anion to metal.

In NaHCO₃ solution, less V_{Fe}^{2-} produces, but so it is easy to meet the requirement of flux:

$$J_{V_{Fe}^{2-}} < J_{Fe_i^{2+}} + J_{V_o^{2+}} \tag{6}$$

The FeCO₃ film is doped by Fe_i^{2+} and V_O^{2+}, and thus it presents n-type semiconductor. In Na₂SO₄ and NaCl solutions, it is easy to generating V_{Fe}^{2-}. Contrarily, the flux is abided by:

$$J_{V_{Fe}^{2-}} > J_{Fe_i^{2+}} + J_{V_o^{2+}} \tag{7}$$

The FeCO₃ film is a p-type semiconductor doped by V_{Fe}^{2-}.

The charge carrier concentration N_q, flat band potential E_{FB} and semiconductor type corresponding to the three solutions are listed in Table 1, where N_q includes donor density (N_D) for n-type semiconductor and acceptor density (N_A) for p-type semiconductor. All the parameters were calculated by linear fitting of Mott-Schottky curves in Fig. 3 based on the equations (2) and (3).

When the n-type or p-type semiconductor contacts with the electrolyte, a conductivity band bending occurs in the semiconductor due to non-uniform

distribution of charge at the interface zone. It can be described by E_{FB}. The E_{FB} is environmental dependent clearly. E_{FB} of n-type semiconductor in $NaHCO_3$ solution is more negative than that of p--type semiconductor in Na_2SO_4 solution and NaCl solution.

The charge carrier concentration reflects the number of defects in the film. It further affects the conductivity of the film due to the transporting of charge carrier. The lowest N_D, 0.27×10^{23} cm^{-3}, was obtained in $NaHCO_3$ solution. The N_A values of 1.72×10^{23} cm^{-3} and 17.2×10^{23} cm^{-3} in Na_2SO_4 solution and NaCl solution were found respectively. The lower N_A in Na_2SO_4 solution should owe to the greater radius of SO_4^{2-} than Cl^-.

It indicated a lower doped semiconductor structure of the film in $NaHCO_3$ solution and a higher doping degree of the film in the other two solutions. The electron passes through the film by the way of flow of doping ions. The higher doping degree the film, the better conductivity is obtained for the film.

Fig. 6 shows the XRD results of the film after immersed in the three solutions. As can be seen, the composition is still $FeCO_3$ (siderite) in each case. According to the mechanism mentioned above, SO_4^{2-} and Cl^- paly role of producing charge carrier and dissolving solid film. They do not participate directly in the substance exchange reaction. For this reason, no matter what the formation water type in the wells containing CO_2, the corrosion scale is mainly composed of $FeCO_3$. The diffraction peak height of film in $NaHCO_3$ solution is stronger than the other two. It means crystal perfection in $NaHCO_3$ solution is the best one, which is clearly observed in Fig.

5.

Relation of semiconducting property and corrosion resistance

Oliveira et al. reported the film gave rise to higher protection when the film changed from p-type to n-type conductor.[13] Different pitting susceptibilities were obtained for the p-type and n-type semiconducting oxide films on the surface of stainless steel.[28] In fact, there should not be direct relation between semiconductor type and corrosion resistance. The corrosion behaviors lie on two important factors, namely, potential and current. They are corresponding to flat band potential and charge carrier concentration.

The potentiodynamic polarization was used to reflect corrosion resistance behaviors of $FeCO_3$ film after immersion in different solutions. The polarization curves were pictured in Fig. 7, and the analysis results were shown in Table 2. After strong polarization, high stable passivity was observed in $NaHCO_3$ solution due to the wide passivation potential range. However, activation polarization presented when high potential was applied in Na_2SO_4 and NaCl solutions, that is to say, passivity was broken down by the aggressive anions of Cl^- and SO_4^{2-}. By the method of Tafel extrapolation, the corrosion currents were calculated by the plots in Fig. 7. They increase with the sequence of $NaHCO_3$, Na_2SO_4 and NaCl solutions. Therefore, HCO_3^- inhibits CO_2 corrosion of N80 steel, but Cl^- and SO_4^{2-}lead to low corrosion resistance. Thus, the protection of $FeCO_3$ film in different solutions decreases with the sequence of $NaHCO_3$, Na_2SO_4 and NaCl. During electrochemical corrosion process,

the anodic reaction, steel dissolution, occurs at steel/film, but the cathodic reaction is always found at film/solution, because the film has more positive potential than the steel itself.[29] The link to cathodic reaction and anodic reaction is electron, i. e, the charge carrier in the film. Higher charge carrier concentration implies rapider electron transfer step. The lowest charge carrier concentration results in passivation in NaHCO$_3$ solution. The charged particles are difficult diffusion. The higher charge carrier concentration drops the IR of film, which accelerates kinetic of corrosion in Na$_2$SO$_4$ and NaCl solutions.

Fig. 8 shows the Nyquist plots of EIS and their equivalent circuits in the three solutions. In Na$_2$SO$_4$ and NaCl solutions, one capacitive loop （semi-circle） was observed, but a Warburg impedance（oblique line）overlapped one capacitive loop in NaHCO$_3$ solution. Warburg impedance is contributed to the transfer resistance of passive film to the conductive ions suggested in the PDM. One capacitive loop without Warburg impedance means the electrochemical reaction at interface between steel and film is the rate control step. The measured data were fitted well by the shown equivalent circuits. Table 3 listed the calculated values of various electrochemical parameters. R$_t$, interface reaction resistant, is inversely proportional to electrochemical corrosion rate. Therefore, the results also prove higher protection of corrosion film in NaHCO$_3$ solution than the other two solutions.

Many works attempted to discover the relationship between E$_{FB}$ and pitting. The apparent phenomenon that lower E$_{FB}$ mitigates susceptibility of pitting nucleation was reported.[30] The decreasing E$_{FB}$ increases band gap energy and pitting potential.

Pagitsas et al.,[31] mentioned that accumulation of V_{Fe}^{2-} due to the incomplete annihilation in reaction (II) exits condensation, and then a large void occurs by a great deal of V_{Fe}^{2-}. The voids weaken the bonding strengthen of film to steel, as a result, the pitting initiates. The vacancy condensation is proportional to the flux of cation vacancy.[20] The adsorbates of some aggressive anions resulting in cation vacancy generation of the deep donor level are mainly responsible for pitting.[32, 33] Cl$^-$ and SO$_4^{2-}$ adsorption answer for the possible pitting.

The quantitative laws between electronic structure and general and pitting corrosion should be further put forward in the future.

4. Conclusions

In order to discover the influence of anions to the physicochemical performance of FeCO$_3$ corrosion film, the film, composed of rhombohedral FeCO$_3$ crystals, was firstly prepared under high temperature and high pressure.

After exposed in the NaHCO$_3$ solution, the FeCO$_3$ film presented an n-type semiconductive character according to the Mott-Schottky measurement. The flat band potential and donor density were -0.31 V$_{SCE}$ and 0.27×10^{23} cm^{-3}. The compact microstructure was maintained. Warburg impedance was observed when EIS was measured. Lowest corrosion current was obtained by fitting the potentiodynamic polarization curve.

In the solution dissolved with Na$_2$SO$_4$, p-type semiconductor with flat band potential of -0.26 V$_{SCE}$ and acceptor density of 1.72×10^{23} cm^{-3} was obtained for the

$FeCO_3$ film. The loose microstructure was observed. High conductive ions concentration elevated corrosion current.

It was similar to the $FeCO_3$ film in Na_2SO_4 solution, p-type semiconducting property was found in the NaCl solution, but the flat band potential and acceptor density were enhanced to 0.14 V_{SCE} and 17.2×10^{23} cm^{-3}. Also the integrity of microstructure was damaged. The highest corrosion current was presented.

Acknowledgments

References

[1] S. Nešić, *Corros. Sci.*, 2007, **49**, 4308.

[2] I. S. Molchan, G. E. Thompson, R. Lindsay, P. Skeldon, V. Likodimos, G. Em. Romanos, P. Falaras, G. Adamova, B. Iliev and T. J. S. Schubert, *RSC Adv.*, 2014, **4**, 5300.

[3] J. K. Heuer and J. F. Stubbins, *Corros. Sci.*, 1999, **41**, 1231.

[4] J. B. Sun, G. A. Zhang, W. Liu and M. X. Lu, *Corros. Sci.*, 2012, **57**, 131.

[5] Z. Yin, W. Zhao, Z. Bai and Y. Feng, *Surf. Interface Anal.*, 2008, **40**, 1231.

[6] D. Liu, B. Qiu, Y. Tomoe, K. Bando and X.P. Guo, *Mater. Corros.*, 2011, **62**, 1153.

[7] Y. Zhang, X. Pang, S. Qu, X. Li and K. Gao, *Int. J. Greenh. Gas Con.*, 2011, **5**, 1643.

[8] G. F. Lin, M. S. Zheng, Z. Q. Bai and Y. R. Feng, *J. Iron Steel Res. Int.*, 2006, **13**, 47.

[9] K. Gao, F. Yu, X. Pang, G. Zhang, L. Qiao, W. Chu and X. Lu, *Corros. Sci.*, 2008, **50**, 2796.

[10] J. Han and J. W. Carey, *J. Appl. Electrochem.*, 2011, **41**, 1367.

[11] Z. Q. Bai, C. F. Chen,   M. X. Lu and J. B. Li, *Appl. Surf. Sci.*, 2006, **252**, 7578.

[12] G. A. Zhang and Y. F. Cheng, *Electrochim. Acta*, 2010, **55**, 316.

[13] M. C. L. Oliveira, V. S. M. Pereira, O. V. Correa, N. B. Lima and R. A. Antunes, *Corros. Sci.*, 2013, **69**, 311.

[14] Z. Feng, X. Cheng, C. Dong, L. Xu and X, Li, *J. Nucl. Mater.*, 2010, **407**, 171.

[15] Y. Zhang, M. Urquidi-Macdonald, G. R. Engelhardt and D. D. Macdonald, *Electrochim. Acta*, 2012, **69**, 1.

[16] J. K. Xiao, *Chin. J. Geochem.*, 1990, **9**, 169.

[17] C. Ren, X. Wang, L. Liu, H. Yang and N. Xian, *Mater. Corros.*, 2012, **63**, 168.

[18] M. Gao, X. Pang and K. Gao, *Corros. Sci.*, 2011, **53**, 557.

[19] D. D. Macdonald, *Electrochim. Acta*, 2011, **56**, 1761.

[20] Z. Jiang, X. Dai, T. Norby and H. Middleton, *Corros. Sci.*, 2011, **53**, 815.

[21] H. Guo, Y. Li and K. Zhao, *J. Hazard. Mater.*, 2010, **176**, 174.

[22] B. Ter-Ovanessian, C. Alemany-Dumont and B. Normand, *Electrochim. Acta*, 2014, **133**, 373.

[23] M. B. Nemer, Y. Xiong, A. E. Ismail and J. H. Jang, *Chem. Geol.*, 2011, **280**, 26.

[24] H. Tanaka, N. Hatanaka, M. Muguruma, T. Ishikawa and T. Nakayama, *Corros. Sci.*, 2013, **66**, 136.

[25] S. Ningshen, U. K. Mudali, V. K. Mittal and H. S. Khatak, *Corros. Sci.*, 2007, **49**, 481.

[26] J. P. Duthil, G. Mankowski and A. Guisti, *Corros. Sci.*, 1996, **38**, 1839.

[27] B. Deng, Y. Jiang, J. Liao, Y. Hao, C. Zhong and J. Lin, *Appl. Surf. Sci.*, 2007, **253**, 7369.

[28] G. Bianchi, A. Cerquetti, F. Mazza and S. Torchio, *Corros. Sci.,* 1972, **12**, 49.

[29] J. Han, S. Nešić, Y. Yang and B. N. Brown, *Electrochim. Acta*, 2011, **56**, 5396.

[30] M. A. Pech-Canul, M. I. Pech-Canul, P. Bartolo-Pérez and M. Echeverrí, *Electrochim. Acta*, 2014, **140**, 258.

[31] M. Pagitsas, A. Diamantopoulou and D. Sazou, *Electrochem. Commu.*, 2001, **3**, 330.

[32] S. Yang and D. D. Macdonald, *Electrochim. Acta*, 2007, **52**, 1871.

[33] Y. F. Cheng and J. L. Luo, *Electrochim. Acta*, 1999, **44**, 2947.

Table 1 Electrochemical parameters calculated from Mott–Schottky plots

Solution	N_q (cm^{-3})	E_{FB} (V_{SCE})	Semiconductor type
NaHCO$_3$	0.27×10^{23}	-0.31	n
Na$_2$SO$_4$	1.72×10^{23}	-0.26	p
NaCl	17.2×10^{23}	0.14	p

Table 2 Analysis to polarization curves of the FeCO$_3$ film in three solutions

Solution	i_{corr} ($\times 10^{-5}$A cm^{-2})	Characteristic
NaHCO$_3$	7.60	Passive state
Na$_2$SO$_4$	13.5	Active state
NaCl	31.6	Active state

Table 3 Fitted electrochemical parameters in EIS by the equivalent circuits

Solution	R_s ($\Omega \cdot cm^2$)	Q ($\Omega^{-1} \cdot cm^2 \cdot s^{-n}$)	n	R_t ($\Omega \cdot cm^2$)	Z_w ($\Omega^{-1} \cdot cm^{-2} \cdot s^{-0.5}$)
NaHCO$_3$	2.62	$3.66*10^{-3}$	0.73	4047	$3.91*10^{-3}$
Na$_2$SO$_4$	3.79	$1.42*10^{-3}$	0.79	1139	-
NaCl	2.09	$1.55*10^{-3}$	0.80	999.5	-
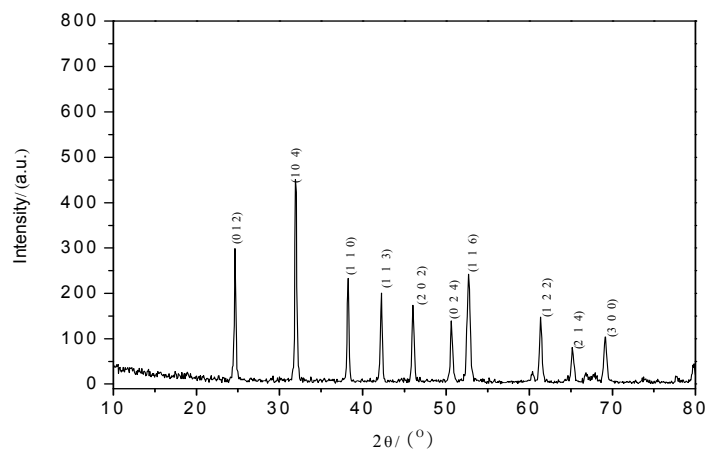
Figure 1. XRD diffraction of corrosion film prepared from CO_2 dissolved water at 90
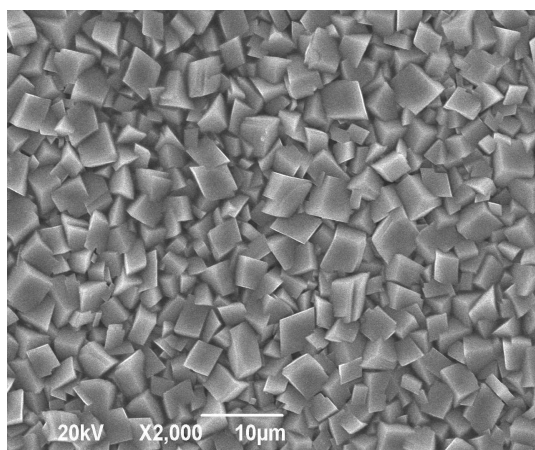
ºC and 8MPa

Figure 2. SEM image of $FeCO_3$ film prepared from CO_2 dissolved water at 90 ºC and

8MPa
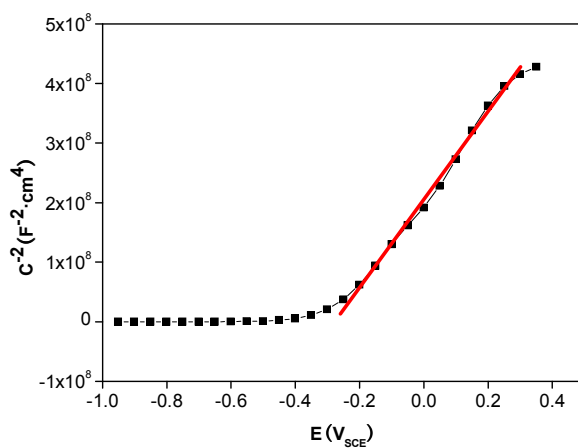
(a) NaHCO$_3$ solution
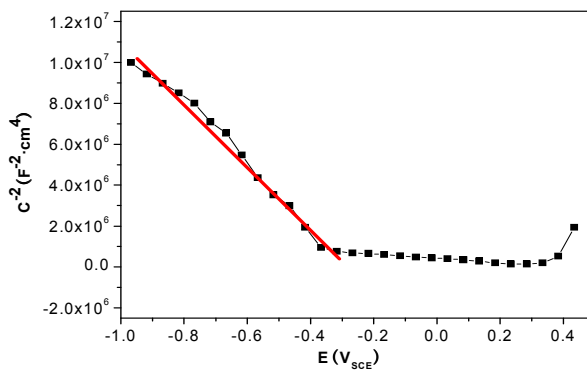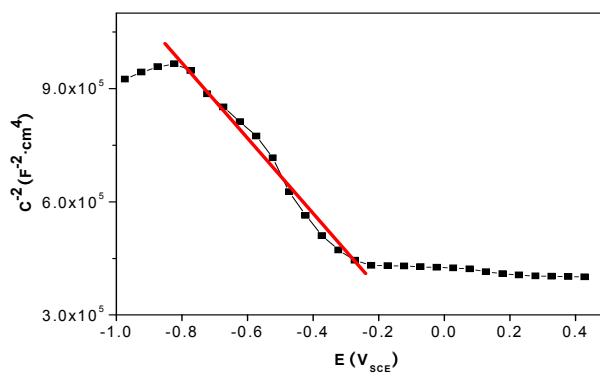
(b) Na$_2$SO$_4$ solution

(c) NaCl solution

Figure 3. Mott–Schottky plots of the FeCO$_3$ film exposed in different solutions
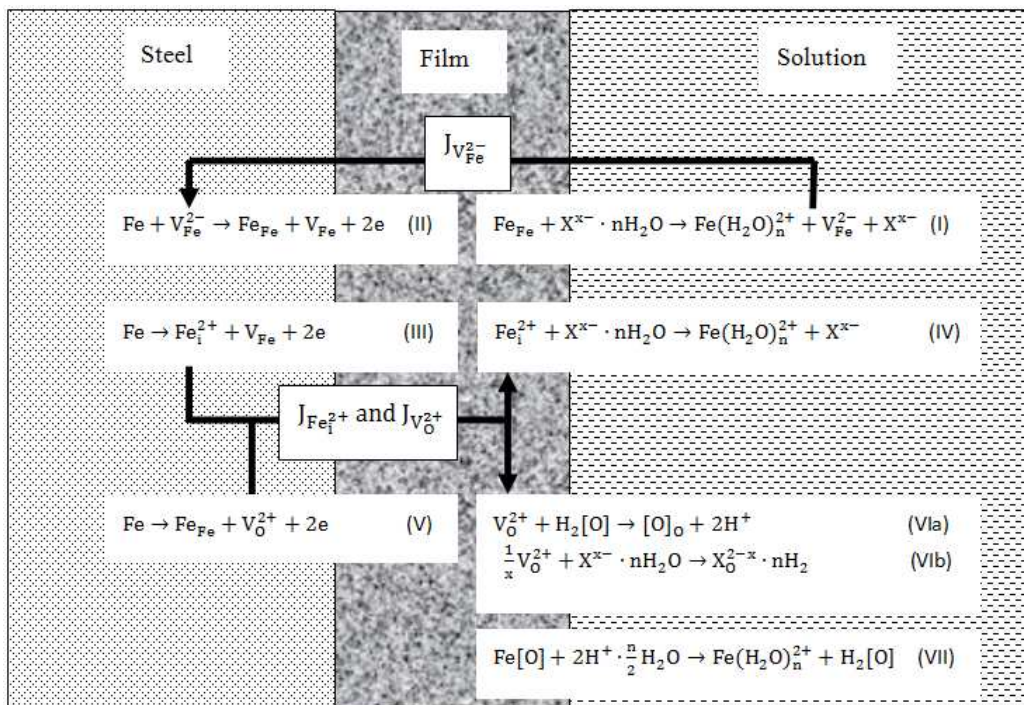
Figure 4. Physicochemical mechanism for the semiconducting type of $FeCO_3$

film
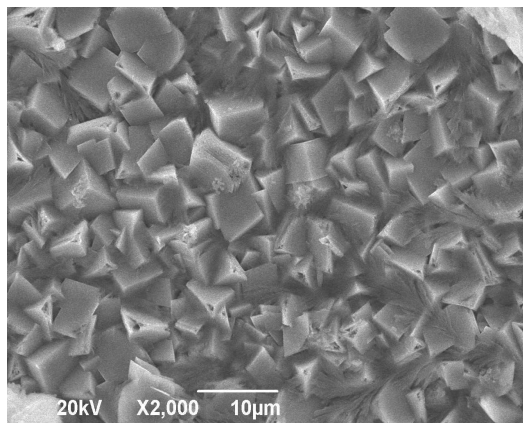
(a) NaHCO$_3$ solution
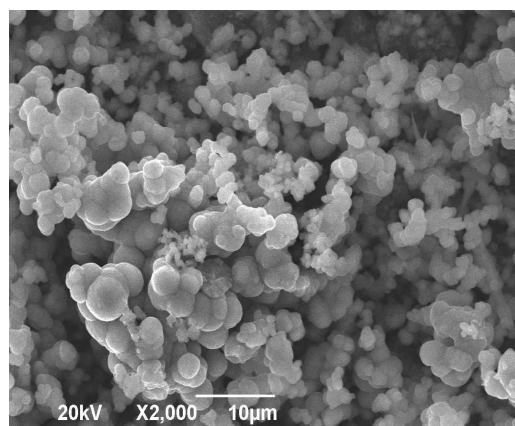
(b) Na$_2$SO$_4$ solution
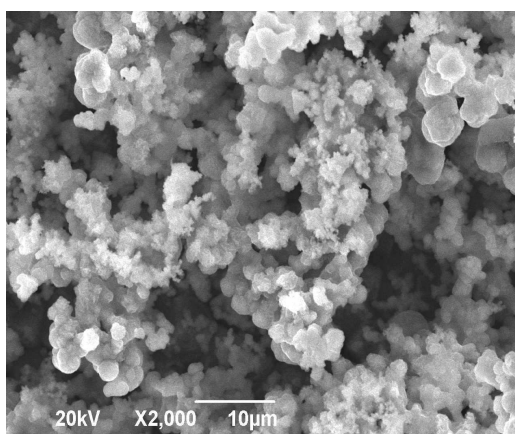
(c) NaCl solution

Figure 5. Surface morphologies of the FeCO$_3$ film after immersing in different
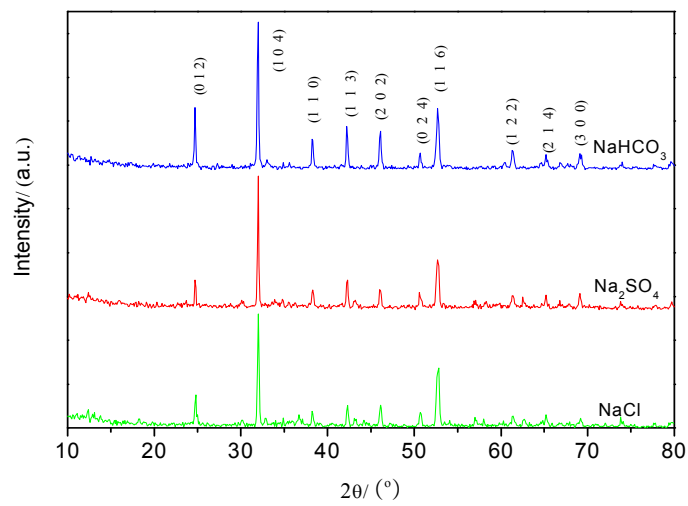
solutions

Figure 6. XRD patterns of the corrosion film after immersing in different solutions
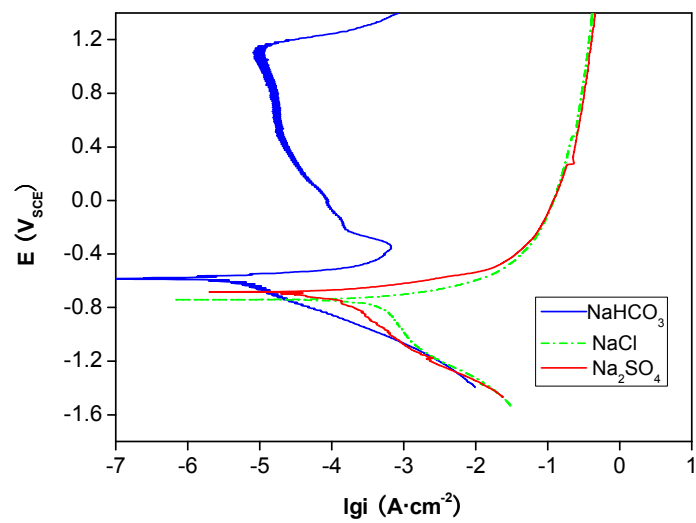
Figure 7. Polarization curves of the FeCO$_3$ film influenced by different solutions
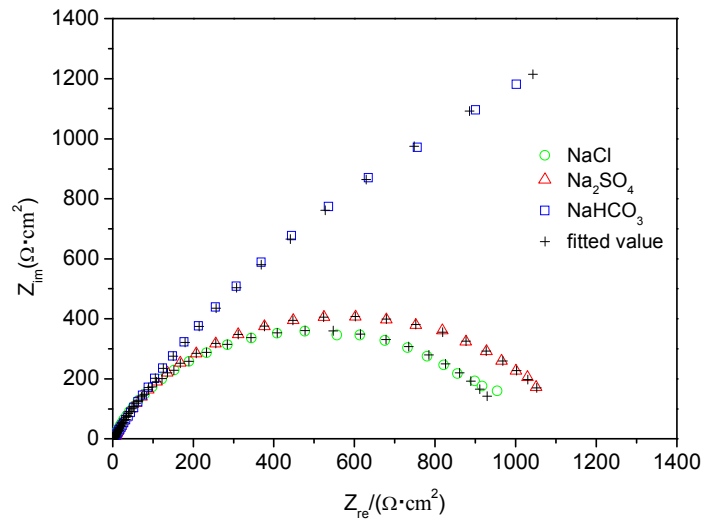
(a) Nyquist plot
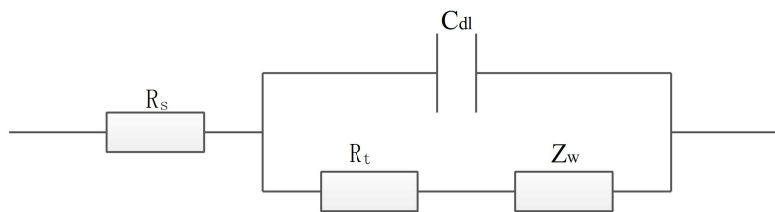
(b) Equivalent circuit in NaHCO$_3$ solution
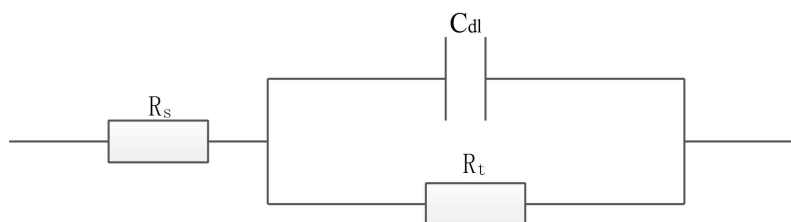
(c) Equivalent circuit in Na$_2$SO$_4$ and NaCl solutions
Figure 8. EIS of FeCO$_3$ film in different solutions